Radiative lifetimes in Ni II

J. E. Lawler and S. Salih
Department of Physics, University of Wisconsin, Madison, Wisconsin 53706
(Received 17 November 1986)

Radiative lifetimes for 12 levels in Ni II are measured using time-resolved laser-induced fluorescence. The lifetimes are used to establish a more accurate absolute scale for earlier transition probability measurements. Issues involved in extending time-resolved laser-induced fluorescence into the vacuum-uv region are discussed.

Time-resolved laser-induced fluorescence on slow atom and ion beams is the most reliable, broadly applicable method for measuring radiative lifetimes. Selective laser excitation eliminates the cascading problem that plagues beam-foil time-of-flight lifetime measurements. The beam environment eliminates errors due to radiation trapping and collisional quenching. We report time-resolved laser-induced fluorescence measurements on Ni II transitions in the uv region ($\sim$200 nm). The Ni II lifetimes are combined with earlier branching-ratio measurements to establish accurate absolute transition probabilities in Ni II. We also discuss problems of extending time-resolved laser-induced fluorescence into the vacuum-uv (vuv) (200—100 nm) region, and some solutions to those problems. The extension of these laser techniques into the vuv region has the potential to provide the laboratory results which will be needed to analyze astronomical observations in the vuv region from the Hubble Space Telescope.[1]

Figure 1 is a schematic of the experiment. The apparatus is a refined version of that used by Duquette *et al.* to produce atomic beams.[2] The fact that the source has produced either an atom or ion beam of 20 different elements is an indication of its versatility and reliability. The beam source is based on a low-pressure, large-bore hollow-cathode discharge. The hollow cathode is used as a beam source by sealing one end of the cathode except for a 1.0-mm-diameter opening. The opening is flared outward at 45° to serve as a nozzle for forming an uncollimated atom or ion beam. The hollow cathode and the scattering chamber are at ground potential. Argon, the sputtering gas, flows continuously into the hollow-cathode discharge. A 10-cm diffusion pump evacuates the scattering chamber. The scattering chamber is sealed from the hollow-cathode discharge, except for the nozzle, and is maintained at a much lower pressure than the discharge. The argon pressure in the discharge is typically 0.3 Torr, while the pressure in the scattering chamber is approximately 10^{-4} Torr.

The most significant change in the ion source from that used for neutral atoms is the addition of a pulsed power supply.[3] The pulsed supply delivers a 5-μsec-duration 16-A-current pulse that produces a burst of metal ions from the source. The discharge current is maintained at 40 mA between pulses by the dc supply.

The ion beam is crossed by a pulsed dye laser beam 1 cm from the nozzle. The dye laser is pumped by a pulsed N_2 laser. The dye laser produces a pulse of 3-nsec duration [full width at half maximum (FWHM)] with a 0.2-cm^{-1} bandwidth and a peak power of up to 40 kW. A KB5 (potassium pentaborate) crystal frequency doubler extends the dye laser tuning range to 217 nm in the ultraviolet region. The fluorescence is detected along an axis orthogonal to both the ion beam and laser beam. In order to minimize scattered light, several sets of light baffles are arranged along the laser beam axis inside the Brewster windows that pass the laser beam into and out of the scattering chamber. Fluorescence from the scattering chamber is focused on the photomultiplier by two lenses comprising an $f/1$ system.

The experiment includes a trigger generator to provide an adjustable delay between the current pulse to the hollow cathode and the laser pulse. The optimum delay of 15 μsec is an average time of flight of the Ni ions. Levels with lifetimes less than 10 nsec are studied in this experi-

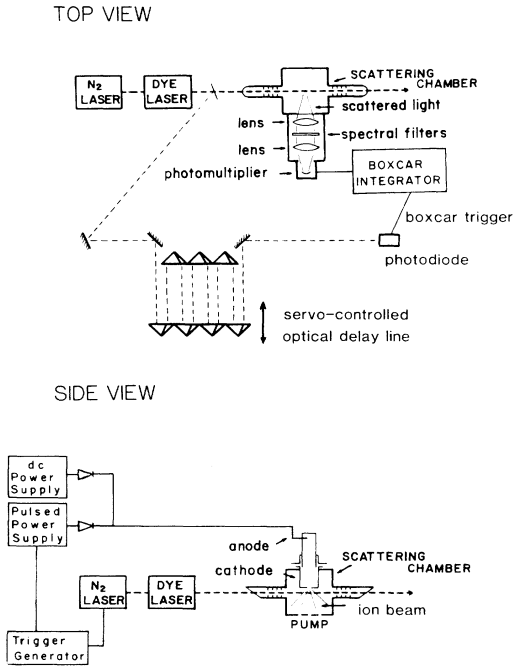

FIG. 1. Schematic of the lifetime experiment.

ment. The average ion velocity of $7\times10^{+4}$ cm/sec, determined by the time of flight, indicates that the ions move less than 7 μm before radiating and essentially no ions leave the 5-mm-long observation region before radiating.

Each radiative lifetime reported in Table I represents an average of at least ten decay curves. The standard deviation of the distribution is typically 5% or less. We believe that the ±0.2-nsec uncertainty is a reliable estimate of total systematic and random error. Laser excitation completely eliminates error due to radiative cascade, because a single fine-structure level is excited using the narrow-bandwidth (0.2 cm^{-1}) dye laser. Collisional quenching is not a problem in this experiment because the scattering chamber pressure is 10^{-4} Torr of argon. Radiation trapping is avoided because the ion beam is optically thin. We discard the first 5 nsec of the fluorescence decay curve. This eliminates any need to deconvolute the fluorescence decay curve from the 3-nsec duration laser pulse. Distortion of the fluorescence decay curve from Zeeman quantum beats is avoided by using coils to zero the magnetic field in the fluorescence collection region to within 0.02 G. The most likely source of systematic error is the finite bandwidth of the detection apparatus.

We discussed the electronic bandwidth of the detection apparatus in some detail in a recent article on Co II.[4] The detection system is composed of a photomultiplier, a delay cable, and a boxcar averager. The bias resistors of the RCA 1P28A photomultiplier are bypassed with capacitors to insure good linearity at large peak currents; small damping resistors are included to reduce ringing. All components are wired for low inductance and fast response. The delay cable is necessary for synchronization of electronic components; it has a risetime of 0.1 nsec. The window width of the PAR 163/165 boxcar integrator is 75 psec. The electronic bandwidth of the entire detection apparatus was tested by measuring the lifetime of $3\,^1P$ and $4\,^1P$ levels of He I.[4] Our measurement of these short and very accurately known He I lifetimes is the primary reason we believe the Ni II lifetimes from this experiment are accurate to ±0.2 nsec.

We made additional improvements in the detection apparatus since the work on Co II.[4] One of the problems in the Co II experiment was due to the limited linearity and accuracy of the electronic time sweep in the scanning boxcar integrator. The manufacturer specifies a linearity of $\pm3\%$ and accuracy of $\pm2\%$ for a sweep of 100 nsec. Approximately 10 nsec of the minimum 100-nsec sweep is used to record a fluorescence decay curve for a 3-nsec lifetime. The linearity and accuracy specifications are not nearly so good for such a short sweep. Although this problem was not discussed in Ref. 4, it did require repeated calibration of the boxcar time sweep with a time mark generator during the Co II work. We avoided using the electronic time sweep in the boxcar integrator in this work on Ni II.

Part of the laser pulse, henceforth called the optical trigger signal, is detected with a very fast *p-i-n* photodiode; the resulting electronic signal is used to trigger the boxcar. The electronic time sweep of the boxcar integrator is replaced with a servo-controlled optical delay line. It introduces a scanable delay in the optical trigger signal. The servo-controlled optical delay line is constructed using seven corner cube reflectors and a surplus *XY* plotter. The optical trigger signal is reflected four times from corner cubes mounted on the moving arm of the *XY* plotter. The surplus plotter provides a smooth, precise

TABLE I. Radiative lifetimes in Ni II.

	Energy (cm^{-1})	λ_{air}[a] (nm)	Lifetime (nsec) This expt. (±0.2 nsec)	KP (Ref. 5)	BPW (Ref. 7) ($+43\%$, -23%)
$3d^8(^3F)4p\ z^4D_{7/2}$	51 558	231.60	3.4	2.5	2.0
$z^4D_{3/2}$	53 635	229.71	3.3	2.5	1.8
$z^4D_{1/2}$	54 176	229.75	3.4	2.5	1.9
$3d^8(^3F)4p\ z^4G_{9/2}$	53 365	227.02	3.2	2.4	2.0
		222.30			
$z^4G_{11/2}$	53 496	221.65	2.9	2.2	1.8
$z^4G_{7/2}$	54 263	226.45	3.2	2.3	1.9
		222.49			
$z^4G_{5/2}$	55 019	225.39	3.0	2.2	1.9
		222.63			
$3d^8(^3F)4p\ z^4F_{7/2}$	55 418	220.67	2.9	2.1	2.0
$z^4F_{5/2}$	56 075	220.14	3.0	2.1	1.9
		217.52			
$z^4F_{3/2}$	56 424	218.46	3.0	2.1	1.9
$3d^8(^3F)4p\ z^2G_{9/2}$	55 300	217.47	3.2	2.5	1.9
$3d^8(^3F)4p\ z^2F_{7/2}$	57 081	229.66	2.9	2.1	2.1

[a]Transition used for laser excitation.

linear motion which is calibrated with a meter stick. This simple device provides linearity and absolute accuracy to better than 1% for time sweeps less than 12 nsec.

Radiative lifetimes deduced from Kurucz and Peytremann's theoretical oscillator strengths are shown in Table I for comparison to our experimental lifetimes.[5] The calculated lifetimes are on the average 26% shorter. Similar comparisons were made in Fe II and Co II. Kurucz and Peytremann's values are shorter than Hannaford and Lowe's experimental Fe II lifetimes by 14%,[6] and are shorter than the experimental Co II lifetimes of Salih *et al.* by 22%.[4] Radiative lifetimes deduced from experimental Ni II transition probabilities of Bell, Paquette, and Wiese are also included in Table I for comparison.[7] Bell *et al.* used the Saha equation and selected Ni I oscillator strengths to establish an absolute scale for their Ni II emission measurements. Their estimated total uncertainty of ±30% on their absolute scale is from several sources including a ±20% uncertainty in the Ni I oscillator strengths, a ±15% uncertainty in the electron density, a ±2% uncertainty in the electron temperature which contributed a ±15% uncertainty to the Ni II absolute scale, and a ±5% uncertainty in spectral calibration between the Ni I and Ni II lines. Their ±30% total uncertainty is actually on the transition probabilities, and if interpreted strictly corresponds to an asymmetric uncertainty of +43%, −23% on lifetimes derived from their transition probabilities. Our accurate lifetimes are on the average 62% longer than those determined by Bell *et al.* using a difficult normalization procedure. The difference is not surprising, is not much longer than their uncertainty, and should not reduce confidence in our measurements. Other absolute transition probabilities measurements on Ni II, including those of Heise,[8] of Goly, Moity, and Weniger,[9] and of Moity,[10] are omitted from Table I. Heise's work included very few lines from levels in this study. Measurements by Goly, Moity, and Weniger,[9] and by Moity[10] lead to lifetimes nearly a factor of 2 shorter than those of Bell, Paquette, and Wiese.[7]

Another interesting comparison involves analogous levels in Fe II, Co II, and Ni II. The terms in the Fe II, Co II, and Ni II $3d^n4p$ configuration which radiate almost exclusively to the $3d^n4s$ configuration, and not to the $3d^{n+1}$ configuration, are those with maximum spin. We might expect that the sum of the emission oscillator strengths from levels in these terms should all be approximately the same. The average total emission oscillator strength $\langle \sum_l f_{ul} \rangle$ from levels in these terms are all 0.25 to within the 5 to 6% accuracy of the laser-induced fluorescence lifetime measurements.[6,4] This comparison includes the Fe II $3d^6(^5D)4p\ z\ ^6D$ levels with $\langle \sum_l f_{ul} \rangle$ equal to 0.257, the Co II $3d^7(^4F)4p\ z\ ^5F$ levels with $\langle \sum_l f_{ul} \rangle$ equal to 0.244, the Co II $3d^7(^4F)4p\ z\ ^5D$ levels with $\langle \sum_l f_{ul} \rangle$ equal to 0.248, the Co II $3d^7(^4F)4p\ z\ ^5G$ levels with $\langle \sum_l f_{ul} \rangle$ equal to 0.261, the Ni II $3d^8(^3F)4p\ z^4D$ levels with $\langle \sum_l f_{ul} \rangle$ equal to 0.236, the Ni II $3d^8(^3F)4p\ z\ ^4G$ levels with $\langle \sum_l f_{ul} \rangle$ equal to 0.247, and the Ni II $3d^8(^3F)4p\ z\ ^4F$ levels with $\langle \sum_l f_{ul} \rangle$ equal to 0.242.

The lifetimes reported in Table I must be combined with branching ratios in order to determine individual transition probabilities. Branching ratios for the Ni II levels were calculated by Gruzdev,[11] and by Mendlowitz.[12] The oscillator strengths calculated by Kurucz and Peytremann are also used to determine branching ratios.[5] Uncertainties on branching ratios from the emission intensity measurements of Bell, Paquette, and Wiese are much smaller than uncertainties on the absolute transition probabilities from those measurement.[7] Branching ratios from these four sources are compared in Table II. Emission intensity measurements by Heise,[8] by Goly, Moity and Weniger,[9] and by Moity[10] are not included in Table II because they are not sufficiently complete to determine branching ratios for many of the levels. The agreement in Table II for branches above 5% is generally good. The theoretical branching ratios bracket the experimental results in most cases. All of the calculations are for intermediate coupling, but they include different numbers of parent terms. The agreement among different theoretical treatments and the experiment is explained by the relatively small configuration mixing in these lowest-lying odd and even parity Ni II levels. We believe that the branching ratios from the measurements of Bell *et al.*[7] are the most reliable and we used them to determine our final gA values in the last column of Table II with a few exceptions. The 232.64-nm transition from the $z\ ^4D_{3/2}$ level is calculated to be an ~11% branch in all three theoretical treatments. The 11% figure also agrees with Moity's measurement.[10] Hence we used 11% for the 232.64-nm branching ratio. The other exception is the vuv transition at 175.19 nm from the $3d^8(^3F)4p\ z\ ^2F_{7/2}$ level to the $3d^9\ a\ ^2D_{5/2}$ level which was not observed by Bell *et al.*[7] We used Kurucz and Peytremann's branching ratio of 13.6% for this transition, and adjusted the other branching ratios of Bell *et al.*[7] for the level proportionally.[5] The number in parentheses following each table entry is an absolute uncertainty in the last digits of the entry. The uncertainty in the gA values includes the uncertainties in the lifetime and the branching ratio.

Laser sources in the vuv are now sufficiently well developed that it is possible to extend time-resolved laser-induced fluorescence experiments into this increasingly important spectral region.[1] Raman-shifted dye laser systems provide complete vuv coverage down to a wavelength of 138 nm.[13,14] Four-wave sum mixing in the rare gases, Hg, or other metal vapors looks promising for even shorter wavelengths.[15] The four-wave-mixing schemes which involve resonant enhancement usually do not provide the broad tunability of stimulated Raman scattering. We constructed a liquid-N_2-cooled Raman cell containing H_2 (or D_2) which is integrated into a Seya Namioka vacuum monochromator.[16] The vacuum monochromator is necessary to separate Raman orders. An integrated design minimizes optical components and thus minimizes losses. The dye laser used to drive the Raman cell is a Nd:YAG pumped dye laser system composed of an oscillator, three amplifiers, and a frequency doubler (YAG represents yttrium aluminum garnet).

The strongest resonance lines in the 300—200-nm uv range are connected to levels with lifetimes of approximately 2 nsec. A comparable oscillator strength at 100 nm indicates a lifetime of 0.5 nsec. Clean, convincing time-resolved laser-induced fluorescence measurements on

TABLE II. Branching ratios and transition probabilities for Ni II. The number in parentheses following a table entry is an absolute uncertainty in the last digit(s) of the table entry.

Upper level energy lifetime	Lower level	λ_{air} (nm)	Branching ratio (%) G (Ref. 11)	M (Ref. 12)	KP (Ref. 5)	BPW (Ref. 7)	gA (10^8 sec^{-1})
$3d^8(^3F)4p\ z\ ^4D_{7/2}$	$a\ ^4F_{9/2}$	231.60	96.3	96.1	96.6	97.2	23.0(14)
51 558 cm^{-1}	$a\ ^4F_{7/2}$	236.74	3.2	2.8	2.3	2.5(1)	0.59(4)
3.4(2) nsec	$a\ ^4F_{5/2}$	241.23	0.23	0.1	0.10	0.08(2)	0.019(5)
	$a\ ^2F_{7/2}$	263.03	0.26	0.2	0.31	0.23(6)	0.054(14)
$3d^8(^3F)4p\ z\ ^4D_{3/2}$	$a\ ^4F_{5/2}$	229.71	89.7	87.7	88.3	82.4(25)	10.8(7)
53 635 cm^{-1}	$a\ ^4F_{3/2}$	232.64	9.8	11.3	10.5	17.6(35)	1.3(4)
3.3(2) nsec							
$3d^8(^3F)4p\ z\ ^4D_{1/2}$	$a\ ^4F_{3/2}$	229.75	100	97.6	98.9	100	5.9(3)
54 176 cm^{-1}	$a\ ^4P_{3/2}$	340.18		1.4	0.12		
3.4(2) nsec							
$3d^8(^3F)4p\ z\ ^4G_{9/2}$	$a\ ^4F_{9/2}$	222.30	24.2	32.9	37.4	31.4(13)	9.8(7)
53 365 cm^{-1}	$a\ ^4F_{7/2}$	227.02	50.8	60.5	50.7	50.0(20)	15.6(12)
3.2(2) nsec	$a\ ^2F_{7/2}$	251.09	25.0	6.6	11.9	18.5(9)	5.8(5)
$3d^8(^3F)4p\ z\ ^4G_{11/2}$	$a\ ^4F_{9/2}$	221.65	100	100	100	100	41(3)
53 496 cm^{-1}							
2.9(2) nsec							
$3d^8(^3F)4p\ z\ ^4G_{7/2}$	$a\ ^4F_{7/2}$	222.49	44.4	44.2	52.0	49.6(20)	12.4(9)
54 263 cm^{-1}	$a\ ^4F_{5/2}$	226.45	47.0	53.2	43.8	45.4(18)	11.4(8)
3.2(2) nsec	$a\ ^2F_{5/2}$	254.59	7.3	1.7	2.9	5.0(3)	1.25(10)
$3d^8(^3F)4p\ z\ ^4G_{5/2}$	$a\ ^4F_{7/2}$	218.81	4.4	1.5	1.9	1.7(2)	0.34(4)
55 019 cm^{-1}	$a\ ^4F_{5/2}$	222.63	37.5	34.5	41.7	38.2(15)	7.6(6)
3.0(2) nsec	$a\ ^4F_{3/2}$	225.39	57.9	63.9	56.1	59.7(42)	11.9(12)
	$a\ ^2F_{7/2}$	241.07	0.03	0.07	0.17	0.34(9)	0.07(2)
$3d^8(^3F)4p\ z\ ^4F_{7/2}$	$a\ ^2D_{5/2}$	180.45[a]			1.7		
55 418 cm^{-1}	$a\ ^4F_{9/2}$	212.59	2.4	2.3	1.6	1.45(6)	0.40(3)
2.9(2) nsec	$a\ ^4F_{7/2}$	216.91	53.4	53.9	45.6	45.7(18)	12.6(10)
	$a\ ^4F_{5/2}$	220.67	34.9	40.6	46.1	48.3(19)	13.3(11)
	$a\ ^2F_{7/2}$	238.78	3.3	2.3	3.2	4.6(3)	1.27(12)
	$a\ ^2F_{5/2}$	247.32	5.9	0.8	1.8		
$3d^8(^3F)4p\ z\ ^4F_{5/2}$	$a\ ^4F_{7/2}$	213.86	6.0	6.8	5.5	5.3(5)	1.06(13)
56 075 cm^{-1}	$a\ ^4F_{5/2}$	217.52	54.4	58.8	52.3	52.8(21)	10.6(8)
3.0(2) nsec	$a\ ^4F_{3/2}$	220.14	37.6	33.3	39.6	39.8(16)	8.0(6)
	$a\ ^2F_{5/2}$	243.36	1.8	0.9	1.5	2.2(1)	0.44(3)
$3d^8(^3F)4p\ z^4F_{3/2}$	$a\ ^4F_{5/2}$	215.87	11.0	12.1	11.1	10.5(16)	1.4(2)
56 424 cm^{-1}	$a\ ^4F_{3/2}$	218.46	89.0	86.4	86.1	87.0(35)	11.6(9)
3.0(2) nsec	$a\ ^2F_{5/2}$	241.30	0.09	1.6	2.2	2.45(10)	0.33(3)
$3d^8(^3F)4p\ z^2G_{9/2}$	$a\ ^4F_{9/2}$	213.13	12.4[b]	1.0	1.0		
55 300 cm^{-1}	$a\ ^4F_{7/2}$	217.47	55.8	21.3	39.0	45.6(18)	14.3(11)
3.2(2) nsec	$a\ ^2F_{7/2}$	239.45	31.8	77.8	59.9	54.4(33)	17.0(15)
$3d^8(^3F)4p\ z^2F_{7/2}$	$a\ ^2D_{5/2}$	175.19[a]			13.6		3.8(9)
57 081 cm^{-1}	$a\ ^4F_{9/2}$	205.33	1.0	0.7	0.9	0.85(7)	0.20(2)
2.9(2) nsec	$a\ ^4F_{7/2}$	209.36	4.0	1.6	1.6	2.2(2)	0.52(6)
	$a\ ^4F_{5/2}$	212.86	8.2	3.8	6.1	8.3(4)	1.98(17)
	$a\ ^2F_{7/2}$	229.66	73.7	71.4	58.7	66.2(26)	15.8(13)
	$a\ ^2F_{5/2}$	237.54	13.1	22.3	19.0	22.4(9)	5.3(4)

[a]Vacuum wavelength.

[b]Gruzdev suspected that the branching ratio is incorrect.

a 0.5-nsec lifetime require (1) a laser pulse which terminates in a time less than 0.5 nsec, (2) a photomultiplier or other sensitive light detector with a response time under 0.5 nsec, (3) and a data logging system of comparable speed.

The laser pulse duration is less important than the abruptness of the pulse termination. A typical transverse pumped dye laser oscillator used with N_2 laser, eximer laser, and Nd:YAG laser pumps has a short and extremely-low-Q cavity. The round trip losses in the 20-cm long oscillator cavity we are using are greater than 99.5%. Only 0.5% of the light survives a round trip in the absence of gain because of the 4% reflection provided by the output mirror, the 26% transmission (double passed) of the prismatic beam expander, and the estimated losses of 50% due to the dye cell and echelle diffraction grating. The high losses are tolerable because of the exceedingly high unsaturated gain provided by the transverse pumped dye cell. The dye laser oscillator thus has negligible capacity to store light. If the pump laser power drops below threshold for the oscillator, then the dye laser output should terminate abruptly. A transverse pumped oscillator of this type is typically followed by one or more amplifiers in order to produce sufficient energy for efficient nonlinear uv and vuv generation. Each nonlinear step, whether frequency doubling in a crystal, frequency summing in a crystal, Raman shifting in a gas, or four-wave sum mixing in a metal vapor, further sharpens the temporal distribution of the pulse. We suggest that substantial additional improvement can be achieved by using a N_2 laser with a subnanosecond pulse duration to pump a short dye laser oscillator, and a standard Nd:YAG laser with a 5—10-nsec-pulse duration to pump the dye laser amplifiers. Compact, high-pressure N_2 lasers which produce subnanosecond pulses are commercially available.

Side-on circular-cage photomultipliers such as the RCA 1P28A have many desirable properties for measuring radiative lifetimes over 2 nsec. They are rugged and inexpensive. They have high gain and are free from ringing when used with a properly designed base which includes damping resistors.[17] Unfortunately they are not sufficiently fast to directly resolve lifetimes in the 0.5—2.0-nsec range. Faster photomultipliers with high gain are available. Some microchannel plate photomultipliers tubes have rise times of 0.25 nsec and pulse widths of 0.5 nsec.[18] A vuv version of one of these should be adequate for most time-resolved laser-induced fluorescence experiments in the 200—100-nm region. The data logging system used in the Ni II experiment should also be adequate in the vuv. The combination of a fast (75 psec) sampling head in the boxcar integrator with the servo-controlled optical delay line is a simple and accurate data logging system for subnanosecond lifetimes. Commercially available transient digitizers, while they capture an entire decay curve each cycle of the experiment, do not have the bandwidth of the fast sampling heads.

Other approaches for detecting and logging the fluorescence include single photon counting with time-to-pulse height conversion, and the use of a streak camera. The former suffers from a low data acquisition rate of ~ 0.1 photon per cycle of the experiment. Such low counting rates are required to prevent distortion of the fluorescence decay curve. If the vuv laser has a low duty cycle then the data collection times become inconveniently long when using photon counting techniques. Commercially available streak cameras with built-in microchannel plate amplifiers have temporal resolution elements as small as 2 psec. Their primary disadvantage, besides cost, is their small effective photocathode area when operated at maximum temporal resolution. This loss of cathode area can probably be offset by using a denser sample of atoms or ions in the laser-induced fluorescence experiment. Dense samples of metallic atoms and ions are available inside of the hollow-cathode discharge.[19] Collisional quenching may be a problem in the discharge or afterglow, but it should be a manageable problem for short lifetimes.

In summary, radiative lifetimes for twelve levels in Ni II are reported. The lifetimes are used to place earlier transition probability measurements on a more reliable absolute scale. Possibilities for extending time-resolved laser-induced fluorescence into the vuv are also discussed. We conclude that time-resolved laser-induced fluorescence techniques can provide important laboratory data in the vuv needed to interpret results from the Hubble Space Telescope.

We wish to acknowledge the support of the National Science Foundation under Grant No. AST85-20413.

[1]S. J. Adelman and D. S. Leckrone, Phys. Scr. **T8**, 25 (1984).
[2]D. W. Duquette, S. Salih, and J. E. Lawler, Phys. Lett. **83A**, 214 (1981).
[3]S. Salih and J. E. Lawler, Phys. Rev. A **28**, 3653 (1983).
[4]S. Salih, J. E. Lawler, and W. Whaling, Phys. Rev. A **31**, 744 (1985).
[5]R. L. Kurucz and E. Peytremann, Smithsonian Astrophysical Observatory Special Report No. 362, 1975 (unpublished).
[6]P. Hannaford and R. M. Lowe, J. Phys. B **16**, L43 (1983).
[7]G. D. Bell, D. R. Paquette, and W. L. Wiese, Astrophys. J **143**, 559 (1966).
[8]H. Heise, Astron. Astrophys. **34**, 275 (1974).
[9]A. Goly, J. Moity, and S. Weniger, Astron. Astrophys. **38**, 259 (1975).
[10]J. Moity, Astron. Astrophys. **64**, 165 (1978).
[11]P. F. Gruzdev, Opt. Spektrosk. **13**, 451 (1962) [Opt. Spectrosc. (USSR) **13**, 249 (1962)].
[12]H. Mendlowitz, Astrophys. J. **143**, 573 (1966).
[13]H. S. Schomburg, H. F. Döbele, and B. Rucke, Appl. Phys. B **30**, 131 (1983).
[14]K. G. H. Baldwin, J. P. Marangos, D. D. Burgess, and M. C. Gower, Opt. Commun. **52**, 351 (1985).
[15]R. Mahon and F. S. Tomkins, IEEE J. Quant. Elect. **QE-18**, 913 (1982).
[16]Liquid N_2 cooling of the SRS cell for improved performance was suggested by R. Van Duyne (private communication).
[17]J. M. Harris, F. E. Lytle, and T. C. McCain, Anal. Chem. **48**, 2095 (1976).
[18]B. Leskovar, Laser Focus/Electro-Opt. **20**, 73 (1984).
[19]P. Hannaford, Contemp. Phys. **24**, 251 (1983).